Talanta 134 (2015) 488–495

Contents lists available at ScienceDirect

Talanta

journal homepage: www.elsevier.com/locate/talanta

# Amperometric uric acid biosensor based on poly(vinylferrocene)-gelatin-carboxylated multiwalled carbon nanotube modified glassy carbon electrode

Pınar Esra Erden [a,*], Ceren Kaçar [a], Funda Öztürk [b], Esma Kılıç [a]

[a] Department of Chemistry, Faculty of Science, Ankara University, Ankara, Turkey
[b] Department of Chemistry, Faculty of Science and Arts, Namık Kemal University, Tekirdağ, Turkey

ARTICLE INFO

*Article history:*
Received 28 July 2014
Received in revised form
15 November 2014
Accepted 22 November 2014
Available online 2 December 2014

*Keywords:*
Amperometry
Uric acid
Biosensor
Poly(vinylferrocene)
Mediator
Carboxylated multiwalled carbon nanotube

ABSTRACT

In this study, a new uric acid biosensor was constructed based on ferrocene containing polymer poly (vinylferrocene) (PVF), carboxylated multiwalled carbon nanotubes (c-MWCNT) and gelatin (GEL) modified glassy carbon electrode (GCE). Uricase enzyme (UOx) was immobilized covalently through *N*-ethyl-*N*′-(3-dimethyaminopropyl) carbodiimide (EDC) and *N*-hydroxyl succinimide (NHS) chemistry onto c-MWCNT/GEL/PVF/GCE. The c-MWCNT/GEL/PVF composite was characterized by scanning electron microscopy, cyclic voltammetry and electrochemical impedance spectroscopy. Various experimental parameters such as pH, applied potential, enzyme loading, PVF and c-MWCNT concentration were investigated in detail. Under the optimal conditions the dynamic linear range of uric acid was $2.0\times10^{-7}$ M – $7.1\times10^{-4}$ M ($R$=0.9993) with the detection limit low to $2.3\times10^{-8}$ M. With good selectivity and sensitivity, the biosensor was successfully applied to determine the uric acid in human serum. The results of the biosensor were in good agreement with those obtained from standard method. Therefore, the presented biosensor could be a good promise for practical applications in real samples.


## 1. Introduction

The rapid, accurate, reliable and inexpensive detection of uric acid in human biological fluids is of great importance in the diagnosis and treatment of several disorders such as gout [1], renal disease [2] and Lesch-Nyhan syndrome [3]. The normal level of uric acid in serum is between 240 and 520 μM [4]. Elevated levels of uric acid in serum are known as hyperuricemia and hyperuricemia has been found to be associated with hypertension [5], metabolic syndrome [6] and cardiovascular disease [7]. Many techniques such as, fluorescence [8], spectrophotometry [9], HPLC-mass spectrometry [10], ion chromatography [11], colorimetry [12], chemiluminescence [13], electrochemistry [14] and electrochemical biosensors [15] have been reported for uric acid detection. Among these techniques, amperometric biosensors provide advantages such as high selectivity and sensitivity, direct measurement, low cost and rapid response [16].

Carbon nanotubes (CNTs) are interesting type of the carbon derivatives offering unique geometrical, mechanical, electronic and chemical properties. CNTs have been extensively researched for sensing applications including fabrication of biosensors because of excellent electrical properties, high surface-to-volume ratio, and high chemical stability. Moreover, CNTs can be used for promoting electron-transfer between the electroactive species and electrode [17]. However, the major challenge for the preparation of CNTs-modified electrodes is the homogeneous dispersion of CNTs since the CNTs form large bundles due to strong van der Waals interactions [18]. Several methods have been investigated to get homogenous dispersion of CNTs [18,19]. Gelatin is a protein obtained from collogens by partial hydrolysis. Because of its many merits, such as its biological origin, biodegradability, nontoxicity, biocompatibility, film forming ability and commercial availability at low cost gelatin has been widely used in food and pharmaceuticals industry [20]. Gelatin also serves as a matrix for the assembly of biomolecules, nanoparticles and other substances [21]. Gelatin was used as an dispersive agent to obtain stable MWCNT dispersions [22,23]. Zheng and Zheng reported that the CNTs-gelatin dispersion was found to be stable for at least two weeks. This good stability was attributed to the immobilization of the non-polar amino acid chain of the gelatin in the side wall of CNTs through hydrophobic–hydrophobic interactions [23]. In this study, gelatin is selected to suspense CNTs owing to its favourable properties mentioned above.

Poly(vinylferrocene) is a conducting redox polymer that contains localized sites that may be oxidized and reduced. PVF is

* Corresponding author. Tel.: +90(312)2126720x1278; Fax: +90(312)2232395.
*E-mail address:* erdenpe@gmail.com (P.E. Erden).

http://dx.doi.org/10.1016/j.talanta.2014.11.058
0039-9140/

widely used as a fundamental system for modeling modified electrode polymer/electrolyte interfaces due to its simple electrochemistry (a reversible one electron process), high stability and the ease of coating of thin film using a variety of methods [24]. PVF was reported as a redox mediator for the oxidation of enzymatically produced hydrogen peroxide [25]. The use of PVF as an immobilization matrix for enzymes such as cholesterol oxidase, creatinase, sarcosine oxidase and urease has been reported in biosensor applications [25–27]. In these biosensors the oxidized form of the polymer ($PVF^+$) was used to bind/immobilize negatively charged enzymes electrostatically above the isoelectric point of the enzymes. The use of PVF as a redox mediator in carbon paste electrodes was also reported [28,29]. In our previous work [26] we have immobilized creatinase and sarcosine oxidase electrostatically onto $PVF^+$ coated Pt electrode to construct an amperometric creatine biosensor. However, the storage stability of this biosensor was not satisfactory due to the weak interaction between the polymer matrix and enzymes. In order to achieve an increased lifetime stability of enzyme electrode, covalent linking of the enzymes on transducer is an efficient method of immobilization [30].

This article describes the fabrication of the uric acid biosensor based on carboxylated multiwalled carbon nanotubes, redox polymer PVF and covalently linked uricase. In previous articles, $[Fe(CN)_6]^{3-}$ [31], 5-methylphenazinium (MP) and 1-methoxy-5-methylphenazinium (MMP) [32] were reported to work as an electron acceptor for UOx in place of $O_2$. In this article, ferrocene containing polymer PVF was used as an useful electron acceptor for UOx. The experimental conditions and the performance parameters of the uric acid biosensor were studied. The successful application of the purposed biosensor for uric acid biosensing in real samples was also described.

## 2. Experimental

### 2.1. Equipment and reagents

The electrochemical studies were carried out using IVIUM electrochemical analyzer (Ivium Technologies, Netherlands) connected to a three-electrode cell stand (Bioanalytical Systems, Inc., USA). The working electrode was a modified glassy carbon electrode (BAS MF 2012). The counter and the reference electrodes were a Pt wire (BAS MW 1034) and Ag/AgCl electrode (BAS MF 2052) (Bioanalytical Systems, Inc., USA), respectively. Scanning electron microscopic (SEM) images were recorded on Carl Zeiss AG, EVO® 50 Series. The pH values of the buffer solutions were measured with ORION Model 720 A pH/ion meter and ORION combined pH electrode (Thermo Scientific, USA).

Uricase (E.C.3.5.3.3. from *Arthrobacter globiformis* sp. with a specific activity of 18 Units/mg solid), uric acid, *N*-ethyl-*N′*-(3-dimethyaminopropyl) carbodiimide, *N*-hydroxyl succinimide, gelatin (type A, porcine skin, analytical grade, G-2500), potassium hexacyanoferrate (III), potassium hexacyanoferrate (II) trihydrate, vinylferrocene and ascorbic acid were supplied from Sigma – Aldrich. Sodium monohydrogenphosphate, sodium dihydrogenphosphate and glucose were from Fluka. Carboxylated multiwalled carbon nanotubes (outer diameter $<8$ nm and length $10-30$ μm) were from Cheaptubes Inc. (Brattleboro, USA). All other chemicals were obtained from Merck. All aqueous solutions

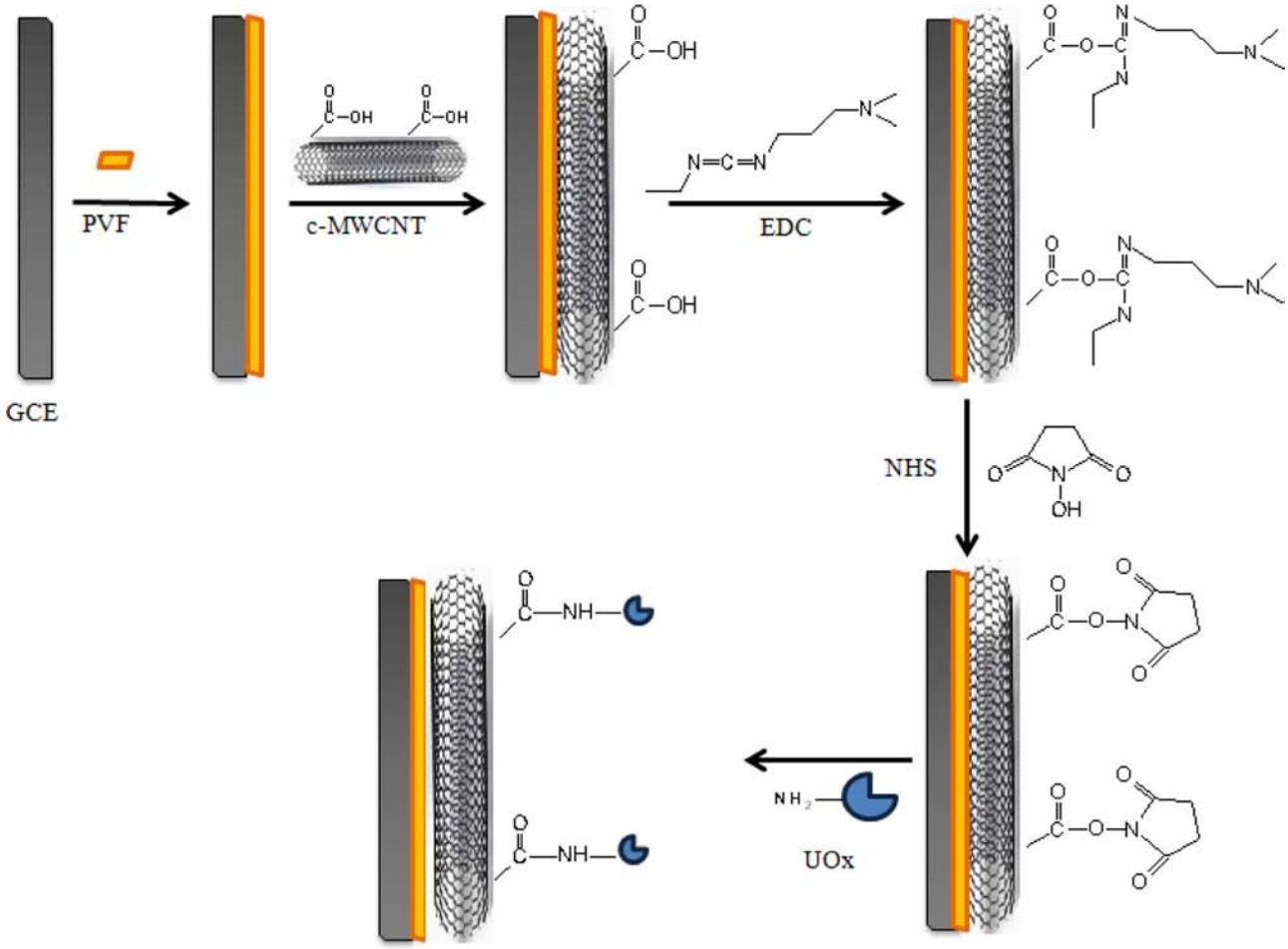


**Scheme 1.** The stepwise fabrication process of the biosensor .

were prepared with double distilled water. Standard solution of uric acid was prepared by dissolving uric acid in 4% $Li_2CO_3$ aqueous solution [33]. The standard uric acid solutions were prepared freshly every day and immediately wrapped with aluminium foil to prevent biomolecule degradation. PVF was prepared by the chemical polymerization of vinylferrocene [34].

### 2.2. Preparation of uric acid biosensor

Before modification, the bare glassy carbon electrode was firstly polished with 0.05 μm alumina slurry, and then rinsed thoroughly with double distilled water, followed by ultrasonication in ethanol and double distilled water for 5 min respectively. After these pretreatments, the cleaned GCE was dried in air. 25.0 mg of gelatin was dissolved in 5.0 mL of double distilled water by magnetic stirring after which it was sonicated for 1 h in order to get a clear solution. Carboxylated multiwalled carbon nanotubes were dispersed into gelatin solution by stirring at room temperature and the resulting mixture was ultrasonicated for 2 h, until a homogenous black dispersion containing 0.5 mg $mL^{-1}$ c-MWCNT was obtained. 10 μL PVF solution in methylene chloride (2 mg $mL^{-1}$) was dropped onto the surface of the GCE and dried. 10 μL c-MWCNT/GEL solution was dropped onto the PVF coated surface of GCE and dried. Uricase solution (0.18 Units $\mu L^{-1}$) prepared in 0.05 M pH 8.0 phosphate buffer solution (PBS) was immobilized onto c-MWCNT/GEL/PVF/GCE using EDC−NHS chemistry. 10 μL of 50 mM EDC–200 mM NHS in 0.05 M pH 8.0 PBS was dropped on the surface and left to dry. Finally, 8 μL of UOx solution was dropped on the top of the electrode and left to dry for 1 h. The biosensor was immersed in 0.05 M PBS (pH 8.0) to wash out the unbound components from the electrode surface. The modified electrodes were kept at +4 °C when not in use. The stepwise fabrication process of the biosensor is shown in Scheme 1.

### 2.3. Electrochemical measurements

Electron transfer properties of the electrodes were examined by cylic voltammetry (CV) and electrochemical impedance spectroscopy (EIS). The CVs of GCE and modified electrodes were recorded between (0)V−(+1.00)V. EIS measurements were performed at the frequency range of $10^5$ Hz−0.05 Hz with 10 mV amplitude under open circuit potential ($E_{OCP}$) conditions in 5.0 mM $Fe(CN)_6^{3-/4-}$ solution containing 0.10 M KCl. All other amperometric measurements were performed in phosphate buffer solution (PBS) (0.05 M pH 8.0). All measurements were carried out at room temperature.

## 3. Results and discussion

### 3.1. Morphologies and electrochemical characteristics of modified electrodes

The surface morphology of modified GCEs was investigated by SEM. Fig. 1 presents the typical SEM images of (a) PVF, (b) c-MWCNT/GEL/PVF (c) UOx/c-MWCNT/GEL/PVF modified GCE surface.

Image a shows the microporous structure of PVF film. Image b shows that the c-MWCNTs dispersed in gelatin are uniformly embedded in the microporous structure of PVF. The porous morphology of the resulting composite is suitable for the immobilization of enzymes. The surface of UOx/c-MWCNT/GEL/PVF modified GCE surface (image c) shows a heterogenous morphology revealing the successful immobilization of UOx in the c-MWCNT/GEL/PVF matrix.

EIS can provide useful information on the impedance changes on the electrode surface during fabrication process. Fig. 2 shows the Nyquist plots of the EIS of (a) PVF/GCE, (b) bare GCE (c) c-MWCNT/GEL/PVF/GCE in 5.0 mM $Fe(CN)_6^{3-/4-}$ solution containing 0.10 M KCl. The Nyquist plot of impedance spectra includes a semicircle portion

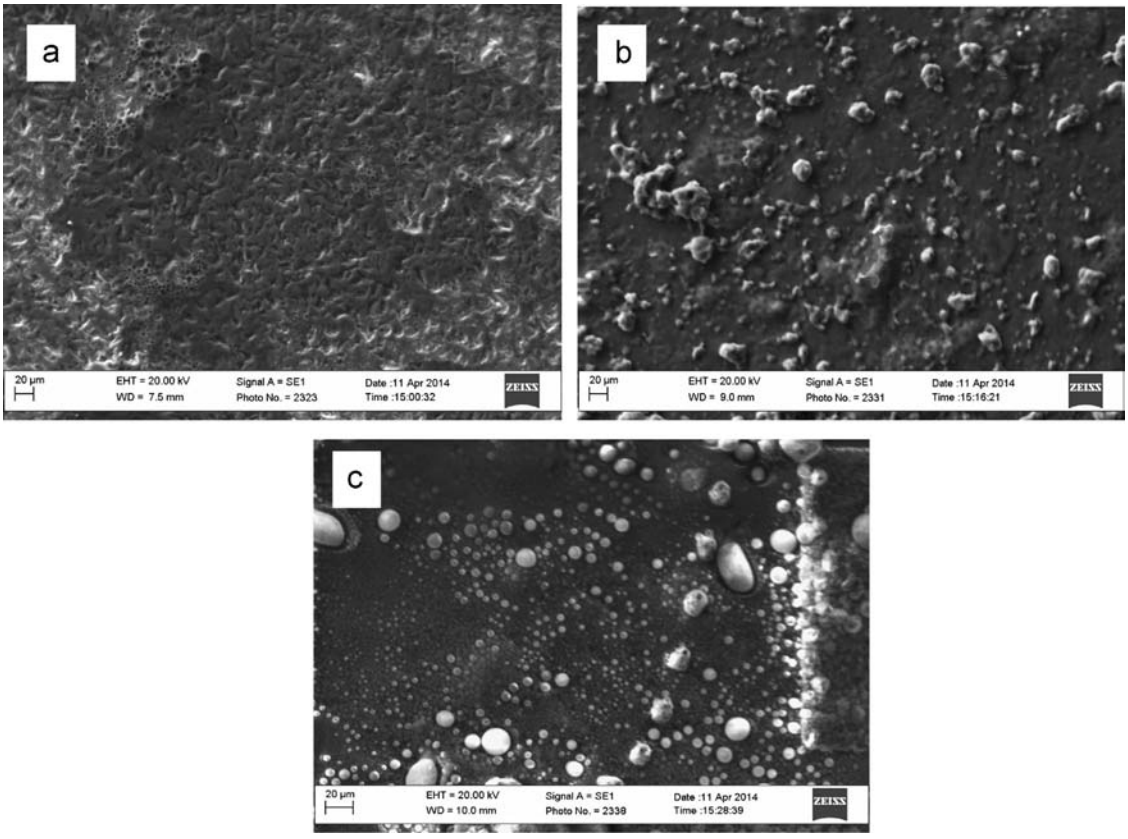


**Fig. 1.** SEM images of (a) PVF, (b) c-MWCNT/GEL/PVF and (c) UOx/c-MWCNT/GEL/PVF modified GCE surface.

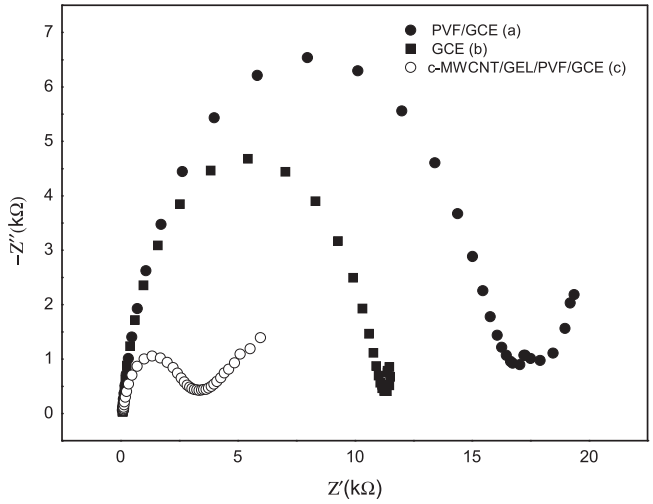


**Fig. 2.** The Nyquist curves of (a) PVF/GCE (b) bare GCE (c) c-MWCNT/GEL/PVF/GCE in 5.0 mM $Fe(CN)_6^{3-/4-}$ containing 0.10 M KCl solution.

and a linear portion. The semicircle portion at high frequencies corresponds to the electron transfer limited process, and the linear portion at low frequencies corresponds to the diffusion process. The diameter of the semicircles is equal to the electron transfer resistance at the electrode surface ($R_{ct}$) [35]. It can be seen from the Fig. 2 that a well-defined semicircle curve was obtained with the bare GCE (curve b). After the electrode was modified with PVF (curve a), the diameter of the semicircle increased suggesting that a layer of PVF was formed on the electrode surface and this layer blocked the diffusion of the redox probe to the electrode surface. After c-MWCNT/GEL composite was covered onto the PVF/GCE, the diameter of the semicircle decreased (curve c), compared with the bare GCE and PVF/GCE. This result may be ascribed to the good conductivity of carboxylated multiwalled carbon nanotubes.

Fig. 3a shows the cyclic voltamogram of PVF coated GCE. PVF/GCE exhibited redox activity due to the coated polymer. The oxidation peak of PVF appears at about +0.49 V versus Ag/AgCl corresponding to a reverse reduction peak of $PVF^+$ with a peak potential of +0.40 V versus Ag/AgCl. It is clear from the figure that the reduction peak is broader and less intense than the oxidation peak. It was reported that neutral PVF polymer takes counter ions into its structure when oxidized and swells. Deswelling occurs upon the reduction of the oxidized polymer as the counter ions are expelled from the structure. The nonidentical swelling and deswelling kinetics of the polymer is the main reason for asymmetry of the anodic and cathodic peaks [36].

Fig. 3b shows the cyclic voltammogram of UOx/c-MWCNT/GEL/PVF/GCE in an 0.05 M pH 8.0 phosphate buffer solution containing 0.10 M KCl without (curve B) and with (curve A) 0.1 mM uric acid solution at scan rate 100 mV $s^{-1}$. It could be seen that with the addition of 0.1 mM of uric acid, the oxidation peak current was increased, which showed the catalytic properties of modified electrode towards the oxidation of uric acid.

Oxygen is the natural electron acceptor for UOx, therefore investigations in the absence and presence of oxygen were performed to determine the mediator effect of PVF (Fig. 4). The removal of oxygen from the solution has no significant effect on the sensitivity of the biosensor when compared with the amperometric response in the presence of oxygen. Hence, it can be concluded that PVF acts as an electron transfer mediator instead of oxygen. It was reported that oxidase-based devices are subject to errors resulting from fluctuations in oxygen tension and the stoichiometric limitation of oxygen since these devices use oxygen as the physiological electron acceptor [37]. Therefore the following experiments were performed under $N_2$ atmosphere. It can be concluded that UOx/c-

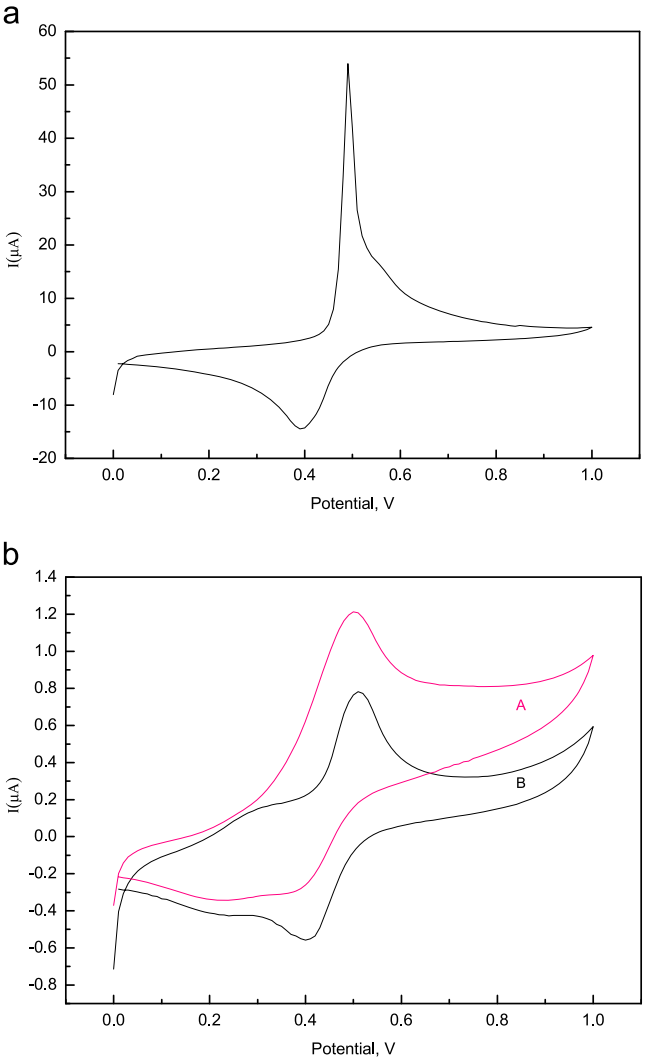


**Fig. 3.** (a) Cyclic voltammogram of PVF/GCE at 50 $mVs^{-1}$, in 0.05 M pH 8.0 phosphate buffer solution containing 0.10 M KCl (b) cyclic voltammogram of UOx/c-MWCNT/GEL/PVF/GCE in an 0.05 M pH 8.0 phosphate buffer solution containing 0.10 M KCl without (curve B) and with (curve A) 0.1 mM uric acid solution at scan rate 100 mV $s^{-1}$.

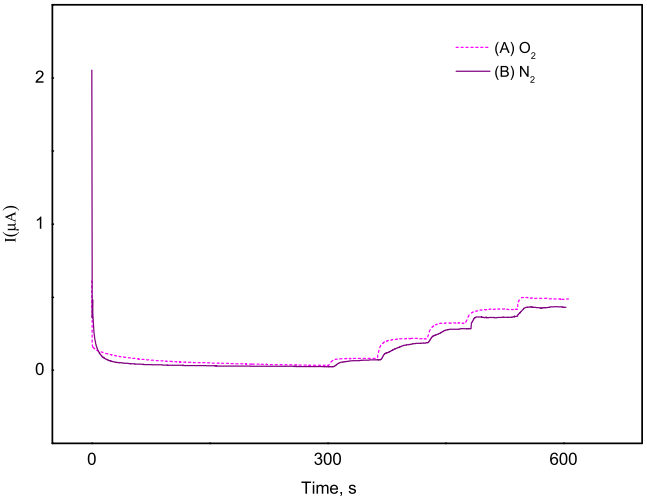


**Fig. 4.** Current–time response of the UOx/c-MWCNT/GEL/PVF/GCE to successive injection of uric acid into a stirred solution of (a) $O_2$ saturated (b) $N_2$ saturated 0.05 M pH 8.0 phosphate buffer at +0.50 V.

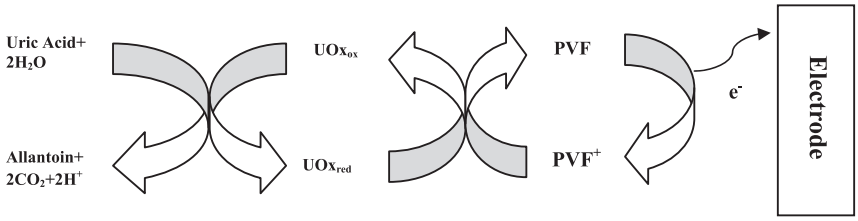


**Scheme 2.** The proposed scheme of biosensor response .

MWCNT/GEL/PVF/GCE provides good performance for uric acid monitoring in oxygen-challenged systems. It was reported that UOx catalyzed oxidation of uric acid may proceed with an ordered mechanism [38]. In this mechanism uric acid and oxygen are bound to UOx to give a trimolecular transitory complex which is dissociated to give the products. In this work we assumed that PVF may work as an electron acceptor instead of dissolved oxygen in the same mechanism. According to the proposed scheme of biosensor action (Scheme 2) $PVF^+$ accepts electrons from the reduced enzyme and PVF is produced. Then PVF is oxidized on the surface of the electrode at +0.50 V versus Ag/AgCl reference electrode. In order to investigate the effect of direct oxidation of uric acid the response of c-MWCNT/GEL/PVF/GCE and UOx/c-MWCNT/GEL/PVF/GCE to uric acid were determined. The sensitivity of UOx/c-MWCNT/GEL/PVF/GCE was found to be two times higher than c-MWCNT/GEL/PVF/GCE. Thus we can conclude that the direct oxidation of uric acid has a contribution to the response of the biosensor.

The electrochemical reactions involved in the response of UOx/c-MWCNT/GEL/PVF/GCE are given below:

$$\text{Uric acid} + 2H_2O \overset{UOX_{(ox)}}{\Longrightarrow} \text{Allantoin} + 2CO_2 + 2H^+$$

$$UOX_{(red)} + 2PVF^+ \rightarrow UOX_{(ox)} + 2PVF$$

$$2PVF \overset{\text{Electrode } (+0.50\ V)}{\Longrightarrow} 2PVF^+$$

### 3.2. Optimization of experimental parameters

The effect of PVF concentration on the response of the biosensor was investigated. PVF concentration was varied between 1 mg $mL^{-1}$ and 3 mg $mL^{-1}$. The response of the biosensor increased with the polymer concentration up to a value corresponding to 2 mg $mL^{-1}$ and then the response current decreased with increasing PVF concentration. This decrease can be attributed to the low diffusion rate of the substrate in the thicker polymer films. The concentration of PVF was kept constant at 2 mg $mL^{-1}$ for all the experiments. The effect of c-MWCNT concentration on the biosensor response was also investigated. The concentration of the c-MWCNT solution ranging from 0.5 mg $mL^{-1}$ to 2 mg $mL^{-1}$ used for the construction of the uric acid biosensor and optimum current response was achieved for 0.5 mg $mL^{-1}$ c-MWCNT. The decrease in the response current of the biosensor at higher c-MWCNT concentrations could be due to an increase in the diffusion barrier. Therefore, 0.5 mg $mL^{-1}$ c-MWCNT concentration was used for further experiments.

To investigate the effect of the enzyme amount on the biosensor response different enzyme loadings were used in the biosensor construction. Four different biosensors were prepared with the UOx loadings varying between 1.1 – 2.2 U and the amperometric responses of the biosensors in 0.05 M phosphate buffer solution containing 0.01 mM uric acid were measured. The current difference increased gradually from 1.1 to 1.4 U and then decreased afterwards. As the maximum current difference was achieved with 1.4 U, this enzyme loading was used for further experiments. The current decrease at higher enzyme loadings may be attributed to the blocking of the electrode surface by the large amount of immobilized protein.

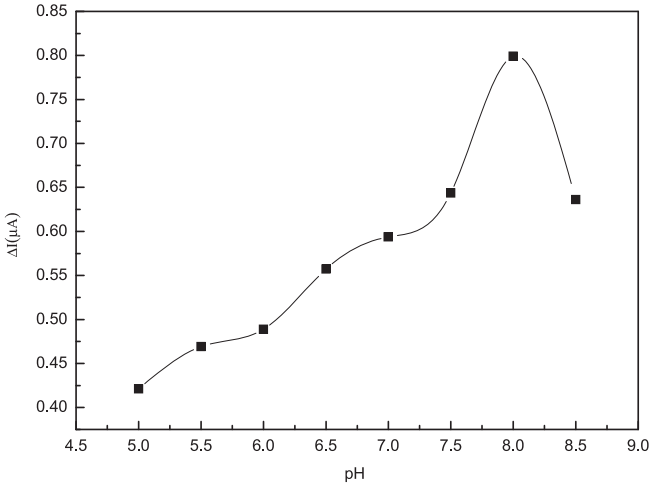


**Fig. 5.** The effect of buffer pH on the response of UOx/c-MWCNT/GEL/PVF/GCE in 0.05 M phosphate buffer containing 0.01 mM uric acid at +0.50 V.

pH of supporting electrolyte is an important parameter affecting the amperometric response of the biosensor. Fig. 5 presents the pH dependence of the amperometric response of 0.01 mM uric acid in the pH range 6.0–8.5. The current differences ($\Delta i$) obtained by the substraction of the background current from the biosensor response. It can be seen that the response current increases with increasing pH value from 6.0 to 8.0, and then decreases as pH increases further. At low pH, the increase in amperometric response with an increasing pH was attributed to the increase of the enzyme activity. As the maximum current difference was achieved at pH 8.0, this pH was considered as the optimized pH for the purposed biosensor. This optimum pH is 0.5 unit less basic than the optimum pH range (8.5–9.2) reported for the free uricase [39]. Such a shift in optimum pH may be attributed to that the microenvironment of the enzyme has been changed by the immobilization, leading to a change of physicochemical characteristics of the enzyme [40].

The influence of applied potential on the response of the biosensor was estimated in 0.05 M pH 8.0 phosphate buffer solution with 0.01 mM uric acid in the range of +0.30 V to +0.60 V. The response current increased as the applied potential shifted from +0.30 V to +0.60 V. Although the highest response was achieved at applied potential of +0.60 V, we have selected the value of +0.50 V for further experiments to minimize the effect of interferences.

### 3.3. Analytical performance of the biosensor

The current response of the UOx/c-MWCNT/GEL/PVF/GCE to uric acid was investigated in $N_2$ saturated 0.05 M pH 8.0 phosphate buffer solution. The amperometric responses at the biosensor for

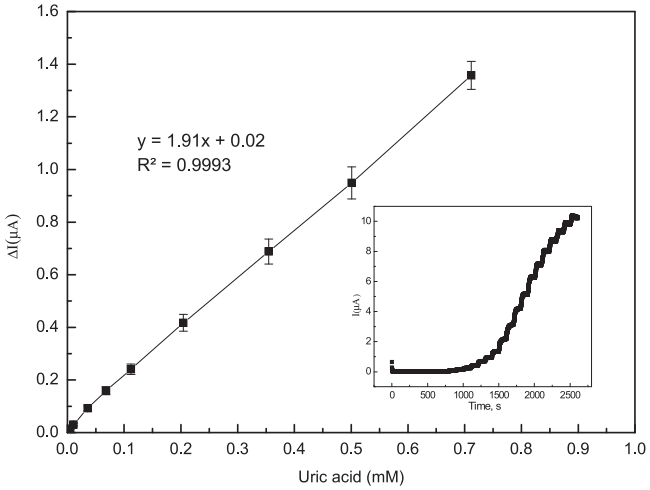


**Fig. 6.** Calibration curve of the UOx/c-MWCNT/GEL/PVF/GCE. Error bars represent the standard deviation for three independent measurements. Inset:Typical current–time response of the biosensor to successive injection of uric acid into a stirred solution of $N_2$ saturated 0.05 M pH 8.0 phosphate buffer at +0.50 V.

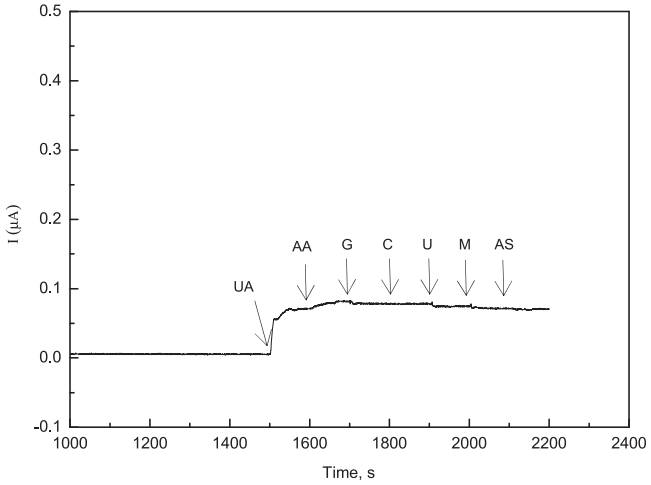


**Fig. 7.** Interference study by successive additions of (a) 0.05 mM uric acid (UA), (b) 0.01 mM ascorbic acid (AA), (c) 0.4 mM glucose (G), (d) 0.01 mM creatinine (C), (e) 0.5 mM urea (U), (f) 0.004 mM metioninine (M), (g) 0.001 mM aspartic acid (AS) in 0.05 M phosphate buffer solution (pH 8.0) at an applied potential of +0.50 V (vs Ag/AgCl).

successive addition of different concentrations of uric acid are presented in Fig. 6 (inset). Upon an aliquot of uric acid was added to the buffer solution, the biosensor responded rapidly to the change of uric acid concentration and reached 95% of steady-state current approximately within 40 s, which was faster than that of 330 s reported at a polypyrrole modified electrode [41], 2 min reported at self-assembled monolayer of 2-aminoethanethiolate on gold electrode [31], 150 s reported at 1,4-benzoquinone modified carbon paste electrode [29]. Response times faster than 40 s were also reported for uric acid biosensors [42,43]. Fig. 6 shows the curve corresponding to the uric acid biosensor. The response of the uric acid biosensor was linear in the range $2.0\times10^{-7}-7.1\times10^{-4}$ M with a correlation coefficient of 0.9993. The detection limit of the biosensor was calculated as $2.3\times10^{-8}$ M from the linear regression method. The linear range of the biosensor is wider than many of those reported in the literature [44–46].

The apparent Michaelis–Menten constant ($K_M^{app}$), a reflection of enzymatic affinity, can be calculated by use of the Lineweaver–Burk equation:

$$\frac{1}{i_{ss}}=\frac{1}{i_{max}}+\frac{K_M^{app}}{i_{max}}x\frac{1}{C}$$

where $i_{ss}$ is the steady-state current after addition of substrate, $i_{max}$ is the maximum current measured under saturated substrate conditions, and C is the bulk concentration of the substrate [47]. The lower $K_M^{app}$ value means that the immobilized uricase possesses higher affinity to uric acid. The $K_M^{app}$ value was calculated to be 0.37 mM which is lower than that for most previous uric acid biosensors [41,44,46] indicating increased affinity of uricase towards uric acid after immobilization.

The repeatability of the UOx/c-MWCNT/GEL/PVF/GCE responses to uric acid was tested by running five sequential calibration curves in the range 0.01 to 0.14 mM. A relative standard deviation (R.S.D.) value of 3.4% was obtained for five successive calibration curves, which indicated a good repeatability of the measurements. Good repeatability of the biosensor may be explained by the fact that the c-MWCNT/GEL/PVF provide a biocompatible microenvironment to maintain the activity of the enzyme. Moreover, the covalent interaction between c-MWCNT and UOx with EDC-NHS is strong and little amount enzyme leaked out from the electrode surface. Long-term storage stability of biosensors is one of the most important factor in case of their commercial use. In this work long−term stability of UOx/c-MWCNT/GEL/PVF/GCE prepared under optimum conditions was investigated by measuring the biosensor response to 0.01 mM uric acid for five weeks. When not in use, the electrode was stored at 4 °C under dry condition. After storage of 10 days the biosensor showed 70% of its original sensitivity. The biosensor showed approximately 50% of its original response after five weeks. The decrease in the response current of the biosensor can be attributed to the time dependent loss of enzyme bioactivity.

To evaluate the selectivity of the biosensor, the influence of some possible interfering substances, such as ascorbic acid, glucose, metioninine, aspartic acid, urea and creatinine was investigated. Amperometric response of the biosensor to successive additions of 0.05 mM uric acid and different concentrations of ascorbic acid (0.01 mM), glucose (0.4 mM), creatinine (0.01 mM), urea (0.5 mM), metioninine (0.004 mM), aspartic acid (0.001 mM) into a stirred solution of 0.05 M pH 8.0 phosphate buffer solution were determined (Fig. 7). Metioninine, aspartic acid and creatinine, which showed no observable change in current were regarded to exhibit no significant effect on the biosensor response. Compared with the response current change of biosensor to uric acid, the relative response current change was approximately 11% for ascorbic acid, 4% for glucose and 2% for urea. When the same analysis was repeated with 10 fold diluted interference concentrations the interference effect of ascorbic acid and glucose decreased to negligable levels. This result demostrates the reliability of the presented biosensor in the determination of uric acid concentration in the presence of interfering species by sample dilution.

A comparison of detection limit, linear range, response time and stability for the presented biosensor with other uric acid biosensors is presented in Table 1. It can be seen that the presented biosensor has favourable analytical performance.

### 3.4. Analysis of real samples

In order to investigate the possible application of this new biosensor in clinical analysis, the modified electrode was tested in real human serum and the results were compared with those obtained by reference method as shown in Table 2.

Enzymatic colour test for the quantitative determination of uric acid in human serum samples was used as reference method. In this technique uric acid is converted by uricase to allontoin and hydrogen peroxide. The trinder reaction is used to measure $H_2O_2$. The formed $H_2O_2$ reacts with N,N-bis(4-sulfobutyl)-3,5-dimethyaniline, disodium salt and 4-aminophenazone in the presence of peroxidase to produce

**Table 1**
Characteristics of various amperometric uric acid biosensors.

| Immobilization matrix/ Immobilization technique | Working potential | Detection limit | Linear range | Stability | Response time | Repeatability (RSD) | pH | Ref. |
|---|---|---|---|---|---|---|---|---|
| Prussian blue nanoparticles, c-MWCNT, polyaniline, gold composite/ chitosan–glutaraldehyde crosslinking | +0.40 V vs Ag/AgCl | 5 μM | 0.005 – 0.8 mM | 37% loss after 7 months | 4 s | 4.6% | 7.5 | [42] |
| RF sputtered NiO thin film deposited on platinum coated glass substrate/ physical adsorption | - | 0.11 mM | 0.05–1.0 mM | About 4 months | 5 s | - | 7.0 | [43] |
| Polyaniline-polypyrrole film/ glutaraldehyte cross-linking | +0.40 V vsAg/AgCl | $1.0 \times 10^{-6}$ M | $2.5 \times 10^{-6}$ - $8.5 \times 10^{-5}$ M | 20% loss after 4 weeks | 70 s | 4% | 9.0 | [44] |
| Tetracyanoquinodimethane modified carbon paste/entrapment | +0.34 V vs Ag/AgCl | $1.9 \times 10^{-7}$ M | $1 \times 10^{-6}$-$1 \times 10^{-4}$ M | 13% loss after 4 months | 70 s | < 1.5% | 8.6 | [45] |
| MWCNT-gold nanoparticle composite/ carbodiimide linkage | +0.40 V vs Ag/AgCl | 0.01 mM | 0.01 – 0.8 mM | 45% loss after 4 months | 7 s | $< 5.6 \pm 0.6$% | 7.5 | [46] |
| SAM of 3-aminopropyltriethoxysilane on ITO/Bis[sulfosuccinimidyl] suberate cross-linking | +0.26 V vs Ag/AgCl | 0.037 mM | 0.05 – 0.58 mM | 15.18% loss after 50 days | 40 – 50 s | 2.5% – 5.1% | 7.4 | [48] |
| Cellulose acetate deposited screen-printed carbon electrode pre-modified with cobalt phthalocyanine | +0.50 V vs Ag/AgCl | 0.015 mM | 0.015 – 0.25 mM | No decrease over the 7-day study period | 180 s | - | 9.2 | [49] |
| Chitosan/Prussian blue prefunctionalized indium-tin oxide/ Langmuir–Blodgett technique | +0.2 V vs. SCE | $1.8 \times 10^{-7}$ | $5 \times 10^{-6}$ M – $1.15 \times 10^{-3}$ M | 20% loss after 2 weeks | 5 – 10 s | 6.8% | 7.0 | [50] |
| ZnO nanoparticles modified MWCNT/ electrostatic binding | +0.32 vs SCE | 2.0 mM | 5.0 μM – 1 mM | 11% loss after 160 days | – | 1.3% | 6.8 | [51] |
| Iron oxide nanoparticles-chitosangraft-polyaniline composite film/covalent immobilization | +0.40 V vs Ag/AgCl | 0.1 μM | 0.1 –800 μM | 10% loss after 100 days | 1 s | 1.58% | 7.5 | [52] |
| PVF-c-MWCNT-GEL composite film/ covalent immobilization | +0.50 V vs Ag/AgCl | $2.3 \times 10^{-8}$ M | $2.0 \times 10^{-7}$ – $7.1 \times 10^{-4}$ M | 30%loss after 10 days | 40 s | 3.4% | 8.0 | This work |

**Table 2**
Comparison of uric acid content in serum samples using the purposed biosensor and enzymatic colour test.

| Serum sample | Reference method concentration (mg/dL) | Proposed method concentration (mg/dL) ± s |
|---|---|---|
| Sample 1 | 4.9 | $5.0 \pm 0.4$ |
| Sample 2 | 3.6 | $3.7 \pm 0.2$ |
| Sample 3 | 4.1 | $4.3 \pm 0.4$ |

s is the standard deviation of 3 experimental values

a chromophore which is read biochromatically at 660/800 nm. The amount of dye formed is proportional to the uric acid concentration in the sample [53].

Serum samples were 150 times diluted. Dilution procedure is important to minimize the interference effects of substances which would come from serum. Standard addition method was used to determine the uric acid concentration in serum sample. In this method, additions of standard uric acid solution were made to several portions of the serum sample, and a multiple addition calibration curve was obtained. The concentration of the uric acid in serum sample was calculated from the calibration curve. Results are in good agreement and show that the presented uric acid biosensor can be used for uric acid determination in serum samples. The accuracy of the method was checked by t-test. The $t$ value is 2.07 for UOx/c-MWCNT/GEL/PVF/GCE at 95% confidence level, for which $t_{critic}$ is 4.30. It can be concluded that there is no difference between the results of two methods at a confidence level of 95%.

## 4. Conclusions

In this study, a novel amperometric uric acid biosensor based on mediator containing polymer poly(vinylferrocene), carboxylated multiwalled carbon nanotubes and covalently linked uricase was successfully developed to detect uric acid in human serum samples. The resulting biosensor exhibited a good analytical performance for the amperometric detection of uric acid, and showed wide linear range, low detection limit and good reproducibility. This favourable analytical performance can be attributed to the following aspects: c-MWCNT/GEL/PVF composite provides a biocompatible microenvironment to maintain the activity of the enzyme. The formation of covalent bond between c-MWCNT and enzyme through EDC-NHS chemistry prevents the leaking of the enzyme. The redox polymer PVF acts as a mediator instead of $O_2$. Moreover, c-MWCNTs provides a conduction pathway to accelerate electron transfer due to their excellent conductivity. The proposed strategy can be extended for the development of other enzyme-based biosensors.

## Conflict of interest

The authors declare that they have no conflict of interest.

## Acknowledgements

We gratefully acknowledge the financial support of Ankara University Research Fund (Project No: 14L0430005).

## References

[1] G.F. Falasca, Clin. Dermatol. 24 (2006) 498–508.
[2] T. Nakagawa, D-H. Kang, D. Feig, L.G. Sanchez-Lozada, T.R. Srinivas, Y. Sautin, A.A. Ejaz, M. Segal, R.J. Johnson, Kidney Int. 69 (2006) 1722–1725.
[3] W.L. Nyhan, J. Inherit. Metab. Dis 20 (1997) 171–178.
[4] C. Retra Raj, T. Ohsaka, J. Electroanal. Chem. 540 (2003) 69 – 77.
[5] F. Jossa, E. Farinaro, S. Panico, V. Krogh, E. Celentano, R. Galasso, M. Mancini, M. Trevisan, J. Hum. Hypertens 8 (1994) 677 – 681.
[6] V. Lohsoonthorn, B. Dhanamun, M.A. Williams, Arch. Med. Res. 37 (2006) 883–889.

[7] J. Fang, M.H. Alderman, JAMA 283 (2000) 2404–2410.
[8] J. Galbán, Y. Andreu, M.J. Almenara, S. Marcos, J.R. Castillo, Talanta 54 (2001) 847 – 854.
[9] D.L. Rocha, F.R.P. Rocha, Microchem. J. 94 (2010) 53–59.
[10] J. Perell´o, P. Sanchis, F. Grases, J. Chromatogr. B. 824 (2005) 175–180.
[11] F.Y. Zhao, Z.H. Wang, H. Wang, R. Zhao, M.Y. Ding, Chinese Chem. Lett 22 (2011) 342–345.
[12] A.K. Bhargava, H. Lal, C.S. Pundir, J. Biochem. Biophys. Meth. 39 (1999) 125 – 136.
[13] F. Wu, Y. Huang, Q. Li, Anal. Chim. Acta 536 (2005) 107–113.
[14] Z. Wang, J. Xia, L. Zhu, F. Zhang, X. Guo, Y. Li, Y. Xia, Sensor Actuat. B. Chem 161 (2012) 131–136.
[15] S. Piermarini, D. Migliorelli, G. Volpe, R. Massoud, A. Pierantozzi, C. Cortese, G. Palleschi, Sensor Actuat. B. Chem 179 (2013) 170–174.
[16] P.E Erden, E Kılıç, Talanta 107 (2013) 312 – 323.
[17] C.B. Jacobs, M.J. Peairs, B.J. Venton, Anal. Chim. Acta 662 (2010) 105–127.
[18] Y.C Tsai, S.Y. Chen, H.W. Liaw, Sensor Actuat. B. Chem 125 (2007) 474–481.
[19] J. Wang, M. Musameh, Y. Lin, J. Am. Chem. Soc. 125 (2003) 2408 – 2409.
[20] Y. Liu, L.M. Geever, J.E. Kennedy, C.L. Higginbotham, P.A. Cahill, G.B. McGuinness, J. Mech. Behav. Biomed. Mater. 3 (2010) 203 – 209.
[21] E. Emregul, O Kocabay, B. Derkus, T. Yumak, K.C. Emregul, A. Sınag, K. Polat, Bioelectrochemistry 90 (2013) 8–17.
[22] A.P. Periasamy, Y.J. Chang, S.M. Chen, Bioelectrochemistry 80 (2011) 114–120.
[23] W. Zheng, Y.F. Zheng, Electrochem. Commun. 9 (2007) 1619–1623.
[24] A. Glidle, A.R. Hillman, K.S. Ryder, E.L. Smith, J. Cooper, N. Gadegaard, J.R.P. Webster, R. Dalgliesh, R. Cubitt, Langmuir 25 (2009) 4093 – 4103.
[25] B.C. Özer, H. Özyörük, S.S. Çelebi, A. Yıldız, Enzyme Microb, Tech 40 (2007) 262 – 265.
[26] P.E. Erden, Ş. Pekyardımcı, E. Kılıç, F. Arslan, Artif. Cell. Blood Sub 34 (2) (2006) 223 – 239.
[27] F. Kuralay, H. Özyörük, A. Yıldız, Sensor Actuat. B. Chem 109 (2005) 194–199.
[28] D. Koyuncu, P.E. Erden, Ş. Pekyardımcı, E. Kılıç, Anal. Lett. 40 (2007) 1904 – 1922.
[29] P.E. Erden, Ş. Pekyardımcı, E. Kılıç, Collect. Czech. Chem. Commun. 76 (2011) 1055 – 1073.
[30] T. Ahuja, I.A. Mir, D. Kumar, Biomaterials 28 (2007) 791–805.
[31] S. Kuwabata, T Nakaminami, S. Ito, H. Yoneyama, Sensor Actuat. B. Chem 52 (1998) 72–77.
[32] T. Nakaminami, S. Ito, S. Kuwabata, H. Yoneyama, Anal. Chem. 71 (1999) 1928 – 1934.
[33] X. Wang, T. Hagiwara, S. Uchiyama, Anal. Chim. Acta 587 (2007) 41 – 46.
[34] W.T. Smith, J. Kuder, E. Wychick, J. Polym. Sci 14 (1976) 2433 – 2448.
[35] J. Wang, Analytical Electrochemistry, John Wiley & Sons Inc. New Jersey, 2006.
[36] Ö. Gökdoğan, M. Sulak, H. Gülce, Chem. Eng. J. 116 (2006) 39 – 45.
[37] J. Wang, Chem. Rev. 108 (2008) 814 – 825.
[38] K. Kahn, P.A. Tipton, Bioelectrochemisty 36 (1997) 4731 – 4738.
[39] E. Miland, M.A.J. Ordieres, T.P. Blanco, M.R. Smyth, C.O Fágáin, Talanta 43 (1996) 785 – 796.
[40] J.D. Qiu, W.M. Zhou, J. Guo, R. Wang, R.P. Liang, Anal. Biochem. 385 (2009) 264–269.
[41] S. Çete, A. Yaşar, F. Arslan, Artif. Cell. Blood Sub 34 (2006) 367 – 380.
[42] R. Rawal, S. Chawla, N. Chauhan, T. Dahiya, C.S. Pundir, Int. J. Biol. Macrom 50 (2012) 112–118.
[43] K. Arora, M. Tomar, V. Gupta, Biosens. Bioelectron. 30 (2011) 333–336.
[44] F. Arslan, Sensors 8 (2008) 5492–5500.
[45] R.F. Dutra, K.A. Moreira, M.I.P. Oliveira, A.N. Araújo, M.C.B.S. Montenegro, J.L.L. Filho, V.L. Silva, Electroanalysis 17 (2005) 701–705.
[46] N. Chauhan, C.S. Pundir, Anal. Biochem. 413 (2011) 97–103.
[47] H. Xu, H. Dai, G. Chen, Talanta 81 (2010) 334–338.
[48] T. Ahuja, D. Kumar Rajesh, V.K. Tanwar, V. Sharma, N. Singh, A.M. Biradar, Thin Solid Films 519 (2010) 1128–1134.
[49] P. Kanyong, R.M. Pemberton, S.K. Jackson, J.P. Hart, Anal. Biochem. 428 (2012) 39 – 43.
[50] X. Wang, F. Yin, Y. Tu, Anal. Lett. 43 (2010) 1507–1515.
[51] Y. Wang, L. Yu, Z. Zhu, J. Zhang, J. Zhu, Anal. Lett. 42 (2009) 775–789.
[52] R. Devi, C.S. Pundir, Sensor Actuat. B. Chem 193 (2014) 608–615.
[53] ⟨https://www.beckmancoulter.com/wsrportal/techdocs?docname=/cis/BAOSR6 × 98/%25%25/EN_URIC%20ACID.pdf⟩.